17th World Conference on Earthquake Engineering, 17WCEE
Sendai, Japan - September 13th to 18th 2020

Comparative Analysis of seismic performance between step-back frame structure and common frame structure

Y. Y. Tang(1), Y. M. Li(2) , S. Y. Ji(3) , L. P. Liu(4)

(1) *Ph.D. Candidate, School of Civil Engineering, Chongqing University, tyyang90@126.com*
(2) *Professor, School of Civil Engineering, Chongqing University, liyingmin@cqu.edu.cn*
(3) *Associate professor, School of Construction Management and Real Estate, Chongqing University, jishuyan@cqu.edu.cn*
(4) *Professor, School of Civil Engineering, Chongqing University, liuliping@cqu.edu.cn*

Abstract

The buildings in mountainous regions are usually constructed with step-back structures regardless of the basis constrained in same height or not, and it has been noticed that this type building suffered severe damages by earthquake in recently years. In order to understand the seismic performance of the step-back frame structure, the response spectrum analysis and dynamic time history analysis of a 6-storey step-back frame structure with 2 floors below upper embedding end, a 6-storey common frame structure and a 4-storey common frame structure were performed respectively. The dynamic characteristic, force and deformation along and across the slope were comparative analyzed from linear elasticity stage to plasticity and failure stages, and the damage status were displayed. The results show that the step-back frame structure has significant torsion effect, and the deformation characteristic of step-back frame structure along the slope is different from that of common frame. The story shear obtained by response spectrum method shows different laws compared with common frame structures at two horizontal directions. Under the action of rare earthquake, the deformation of the 6-storey step-back frame structure is smaller than 6-storey common frame structure. Common frame structures show typical beam hinge mechanisms. In the along-slope direction, the damage mechanisms of step-back frame structure is different from that of common frame. The plastic hinges appear at bottom of upper embedding columns, and the beams and columns at floors below upper embedding end are no damage. In the across-slope direction, the bottom of columns at upper embedding end and lower embedding end are damaged. Under the action of stronger earthquake, the damage mechanisms of step-back frame structure along the slope is slightly different, and plastic hinges appear at beam ends of floor below upper embedding end.

Keywords: step-back frame structure, seismic performance, deformation characteristic, damage mechanisms

1. Introduction

The buildings in mountainous regions are usually constructed with step-back structures regardless of the basis constrained in same height or not, especially these structures have being constructed in mountainous region. According to the observation of the severe damages of buildings destroyed in Wenchuan earthquake and Sikkim earthquake, the structure with foundations at different elevations shows special features different from common structures with foundations at same elevation. The damage of vertical components fixed at highest positions is significantly more severe than the rest, and the torsion effect is remarkable [1-3].

Recently years, more and more attention have been paid on specific characteristic of step-back frame structure. Yao Z [4] studied the relationship between its dynamic characteristics along the slope and the distribution of structural stiffness and mass by simplified analytical model. Cunxiong W [5] carried out research on the redistribution of internal force under great earthquake in the along-slope direction, and some suggestions were proposed for the seismic design. But there is an inevitable torsion effect in this structure because of the noncoincidence of the center of mass and the center of rigid in the across-slope direction [6]. The correlation of seismic response between plane model along the slope and three-dimensional model was conducted, and the result showed that the plane model can't completely represent the actual response of the structure [7]. In order to accurately achieve the seismic performance of step-back frame structure, the analysis on three-dimensional model is necessary.

In this paper, the response spectrum analysis under the action of frequent earthquake and dynamic time history analysis under the action of rare earthquake of three frame structures, a 6-storey step-back frame structure with 2 floors below upper embedding end, a 6-storey common frame structure and a 4-storey common frame, were performed respectively. The dynamic characteristic, force and deformation in the along-slope and across-slope direction were comparative analyzed from linear elasticity stage to nonlinear and failure stages, and the damage status under the action of rare earthquake and more powerful earthquake were displayed. The differences of structural seismic performance between step-back frame and common frame were summarized.

2. Modeling of frame structures

2.1 Structural configurations

A reinforcement concrete step-back frame structure and two corresponding common frame structures are established, and according to the structural arrangement, these structures are named as M-D2K1, M-6 and M-4, as shown in Fig.1. The X axis and Y axis represent the along-slope and across-slope directions. The structures own 3 bays along the slope and 2 bays along the slope. In step-back frame structure, there are 2 floors below upper embedding end and 4 floors above upper embedding end. The corresponding common structures are 6 floors and 4 floors, respectively. The floor height is set constant to 3.0m, and the bay width is 6.0m in two horizontal directions.

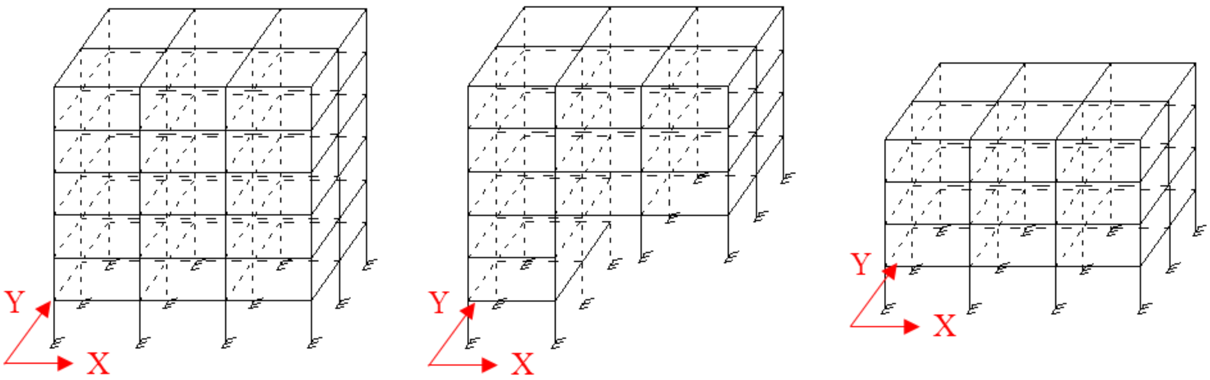

a) M-6 b) M-D2K1 c) M-4

Fig. 1 – Sketch maps of frame structure models

In these frame structures, the thickness of floor slab is 140mm, and there is no secondary beam. The column section is 600mm×600mm, and the beam section is 300mm×600mm. In view of Chinese code GB50009-2012, the additional uniform dead load and the uniform live load are set as 1.5 kN/m^2 and 2.0 kN/m^2 at all floors, and the linear dead load of infilled wall is 9 kN/m. The grade of steel reinforced is HRB400, and the concrete strength grade selected is C30. It is assumed that the basic fortification intensity of the structures is 0.20g, and the predominant period of the site where the structures are located is 0.35s.

2.2 Analysis models and ground motion records

According to the above structural configurations, three-dimensional structural models of the investigated structures are built by analysis and design software YJK2014. The analytical models for dynamic time history analysis are created using PERFOEM 3D. Beams and columns are modeled as frame member compound by inelastic fiber section at two ends and RC section in the middle. The slabs are modeled as rigid diaphragms. The modified Kent and Park constitutive model [8] is used to model concrete behavior. The compressive cylinder strength $f_c^{'}$ and Modulus of elasticity E_c of concrete are taken as 29.14 MPa and 2.98×10^4 MPa, respectively, and the strain at maximum stress of unconfined concrete ε_0 is 0.002. Bilinear model [9] considering an elastic-perfectly plastic (e-p-p) relationship is used to simulate the stress-strain curve of steel in tension and compression. The yield stress f_y and modulus of elasticity E_s of steel reinforced are taken as 452 MPa and 2×10^5 MPa, respectively.

Table 1 – Ground motion records

No.	Magnitude	Year	Earthquake Name	Station Name	Direction	Record Sequence Number
1	7.36	1952	Kern County	Taft Lincoln School	21	15
2	6.19	1966	Parkfield	Cholame - Shandon Array #12	50	28
3	6.53	1979	Imperial Valley-06	Cerro Prieto	147	164
4	6.9	1980	Irpinia_ Italy-01	Sturno (STN)	0	292
5	6.2	1980	Irpinia_ Italy-02	Rionero In Vulture	0	302
6	6.36	1983	Coalinga-01	Parkfield - Gold Hill 4W	0	353
7	6.93	1989	Loma Prieta	APEEL 3E Hayward CSUH	0	734
8	6.93	1989	Loma Prieta	APEEL 9 - Crystal Springs Res	137	736
9	6.93	1989	Loma Prieta	Bear Valley #5_ Callens Ranch	220	746
10	6.93	1989	Loma Prieta	Calaveras Reservoir	90	751
11	6.93	1989	Loma Prieta	Fremont - Mission San Jose	0	762
12	6.93	1989	Loma Prieta	Sunol - Forest Fire Station	90	807
13	7.01	1992	Cape Mendocino	Fortuna - Fortuna Blvd	0	827

Based on the site condition and structures' fundamental natural vibration period [10], 13 ground motion records are chosen from PEER for dynamic time history analysis, and the basic information is shown in Table 1.

3. Dynamic characteristic

Table 2 lists the first six order periods of models. The period of step-back frame structure is between the same order periods of two common frame structures. Fig. 3 and Fig. 4 shows first three mode shape of M-6 and M-D2K1. The mode shape of M-4 is similar with that of M-6, and it will not be presented for sake of brevity. The first mode is only translational motion along Y axis in common structure, while in step-back structure, it is the combination of torsional and translational motion along Y axis. The second mode of M-6 is similar to that of M-D2K1, so does the third mode. It should be noticed that the location of the center of twist in third mode is different.

Table 2 – Periods of frame structures

Model	T1(s)	T2(s)	T3(s)	T4(s)	T5(s)	T6(s)
M-6	0.758	0.729	0.616	0.234	0.227	0.192
M-D2K1	0.579	0.502	0.425	0.191	0.164	0.134
M-4	0.479	0.463	0.391	0.144	0.140	0.119

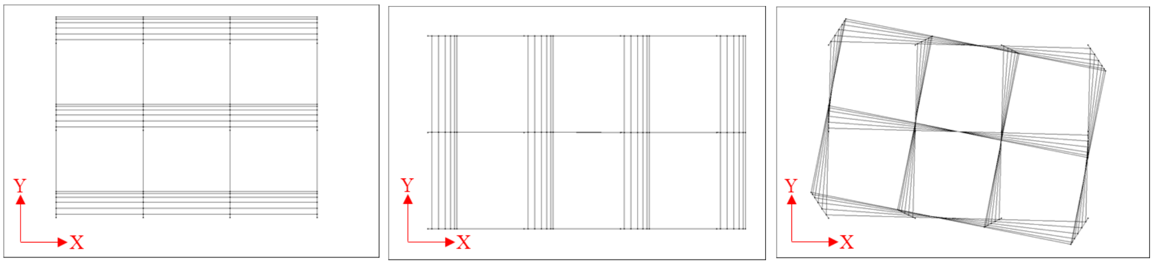

a) 1st mode shape b) 2nd mode shape c) 3rd mode shape

Fig. 2 – Mode shapes of M-6

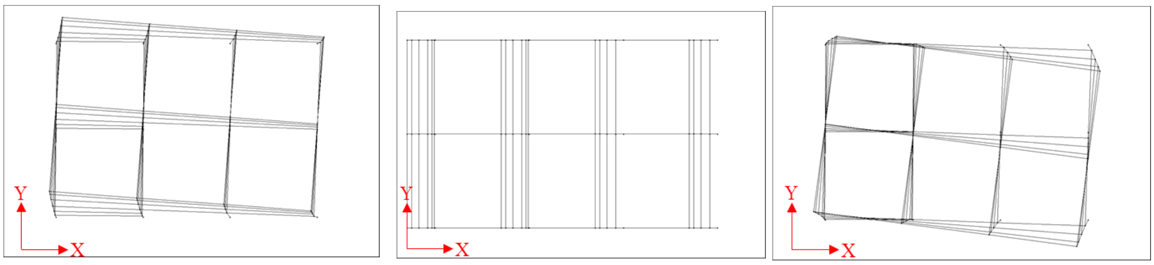

a) 1st mode shape b) 2nd mode shape c) 3rd mode shape

Fig. 3 – Mode shapes of M-D2K1

4. The force and deformation

Fig. 4 presents the distribution of seismic action and shear force of frame structures. In this section, the floor number of structure M-4 starts from 3 for the convenience of comparing. It can be observed that the seismic action of common frames M-6 and M-4 conform to the distribution law of inverted triangle along X-axis and Y-axis except for the top floor. In step-back frame structure M-D2K1, the increasing trend of seismic action at floors below upper embedding end (1st floor and 2nd floor) is weaker than floors above upper embedding end (from 3rd floor to 5th floor), especially in along-slope direction. The shear force of three frame structures show a gradual increase from top floor to 3rd floor, and the value is close to one another. At the 1st and 2nd floor, shear force of M-6 keeps increasing, while there is an abrupt decrease of shear force at 2nd floor in structure M-D2K1, which results from the load transmission of columns connected with upper embedding end. The shear force of floors below upper embedding end along the slope is significantly less than that across the slope.

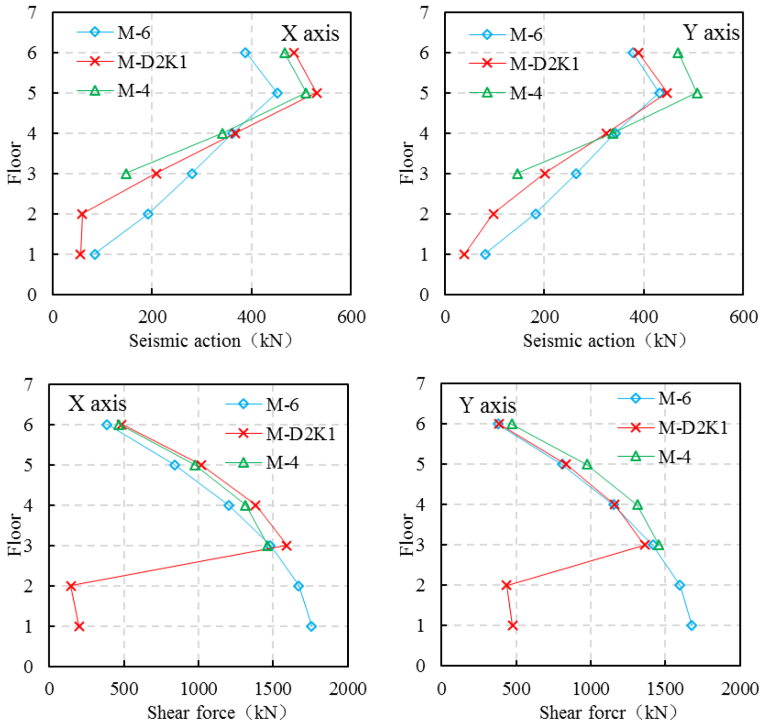

Fig. 4 – Seismic action and shear force of frame structure models by response spectrum analysis

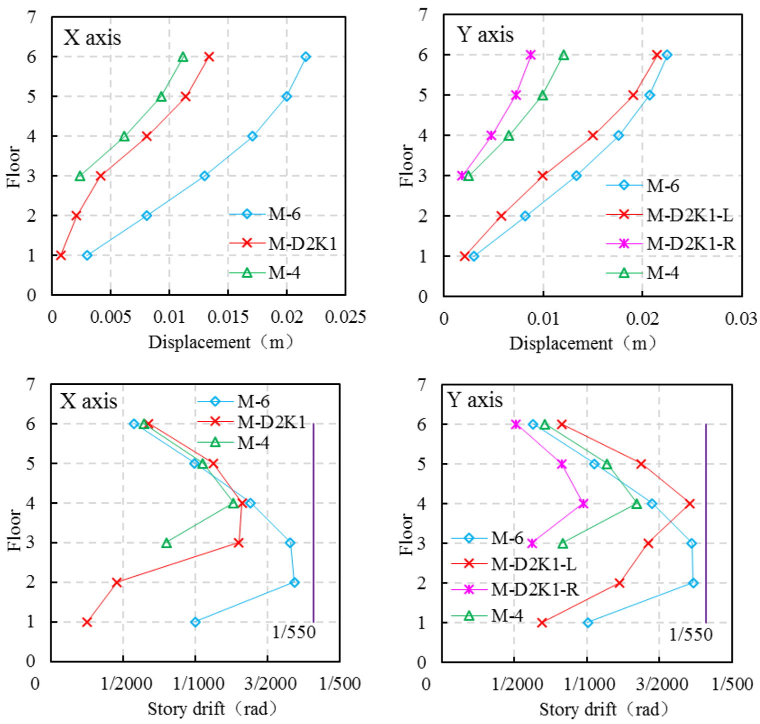

Fig. 5 – Displacement and story drift of frame structure models by response spectrum analysis

Fig. 5 shows the displacement and story drift of frame structure models under frequent earthquake by response spectrum analysis, in which M-D2K1-L represents the side of columns connected with lower embedding end and M-D2K1-R represents the side of columns connected with upper embedding end. The displacement of M-D2K1 is between that of M-4 and M-6 at the direction along the slope, and the deformed shape is different from common frame structure, which is limited to some extent at floors below upper embedding end. Because of torsion effect, the displacement of M-D2K1 is different on both sides across the slope. The displacement across the slope is less than that of common frame with same height.

The maximum story drifts of the investigated structures are less than the limit value 1/550 defined by Chinese code GB 50011-2010. In the along-slope direction, the story drift of M-D2K1 is close to that of common frame from 4th floor to 6th floor, and less than that of common frame from 1st floor to 3rd floor, which is consistent with the limitation of displacement at these floors. In the across-slope direction, except for the story drift of M-D2K1-L from 4th floor to 6th floor, the story drift of step-back frame structure is evidently less than that of common structure. The maximum story drift of M-D2K1 along the slope is obviously less than that of M-6, and the values of two models across the slope are approximate to each other. The floor on which the maximum story drift is located is 4th floor in M-D2K1, which is different from M-6.

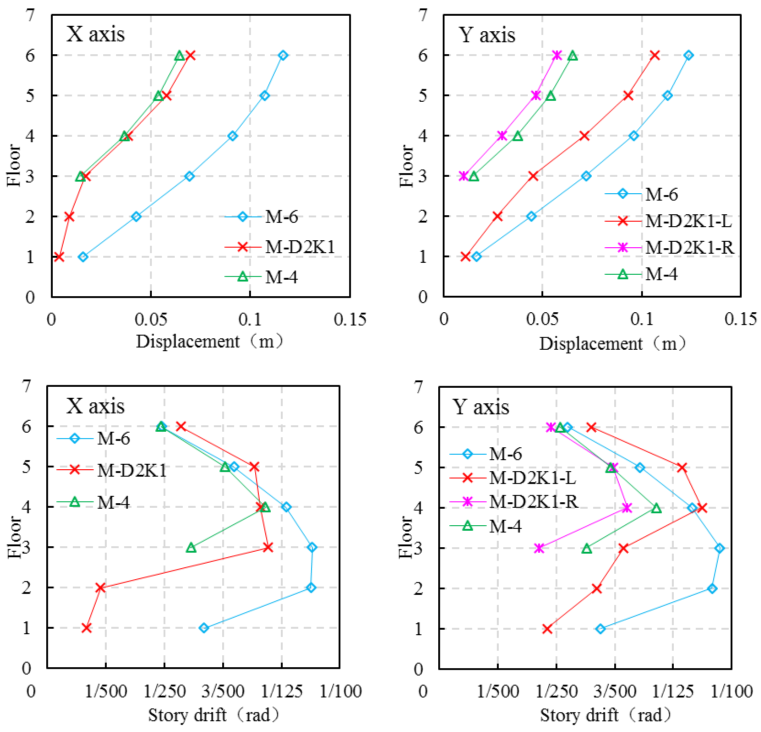

Fig. 6 – Displacement and story drift of frame structure models by dynamic time history analysis

The average displacement and average story drift of frame structure models by dynamic time history analysis under rare earthquake are shown in Fig. 6. The deformation rule is similar to the result of corresponding structure obtained by response spectrum analysis shown in Fig. 5. The deformation of M-D2K1 along the slope is closer to M-4 compared with M-6. The maximum story drifts of M-D2K1 in the along-slope and across-slope direction are less than the corresponding values of M-6, and the maximum story drift is located on 3rd floor in the along-slope direction.

5. The plastic hinges

The maximun shear force V of each column under rare earthquake and its shear capacity V_u can be achieved, and there is $V < V_u$ for all columns, which means that no shear failure happens in columns. Bending failure is showen in this section. Ductility coefficient of sectional curvature is always adopted to indicate the degree of plastic hinge. When ductility coefficient of sectional curvature of the beam or column is greater than 1, plastic hinge is developed. The plastic hinges of the structure are not the same under the action of every ground motion record selected, but the basic laws are all alike. So just the results under the action of ground motion record 13 are displayed for brevity.

Plastic hinges of frame structure models under rare earthquake with intensity of 0.40g along X axis are displayed in Fig. 7, and the degree of plastic hinge is divided into three levels. It can be observed that plastic hinges are mainly at the end of columns and beams along X axis, and the distribution is basically symmetric about the X axis. In common frame structure M-6, the majority of plastic hinges are located at beams ends, and there are plastic hinges at the bottom of small part columns at 1st floor. In M-4, the bottom of columns at 1st floor are all hinged, and some plastic hinges occur at the top of columns at 2nd floor. Common frame structures show typical beam hinge mechanisms. In step-back frame structure M-D2K1, there is no plastic hinge at components' end at floors below upper embedding end. The bottom of columns connected with upper embedding end are all hinged, and plastic hinges develop at the top of more than half of columns at 5th floor. The damage degree of beams in M-D2K1 is graeter than that in M-4 and M-6.

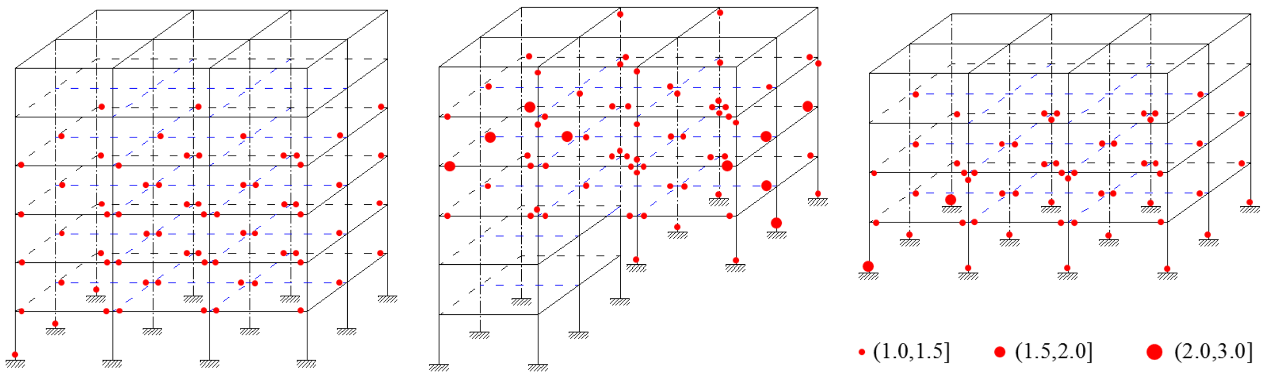

a) M-6 b) M-D2K1 c) M-4

Fig. 7 – Plastic hinges of frame structure models under the action of ground motion record 13 with intensity of 0.40g along X axis

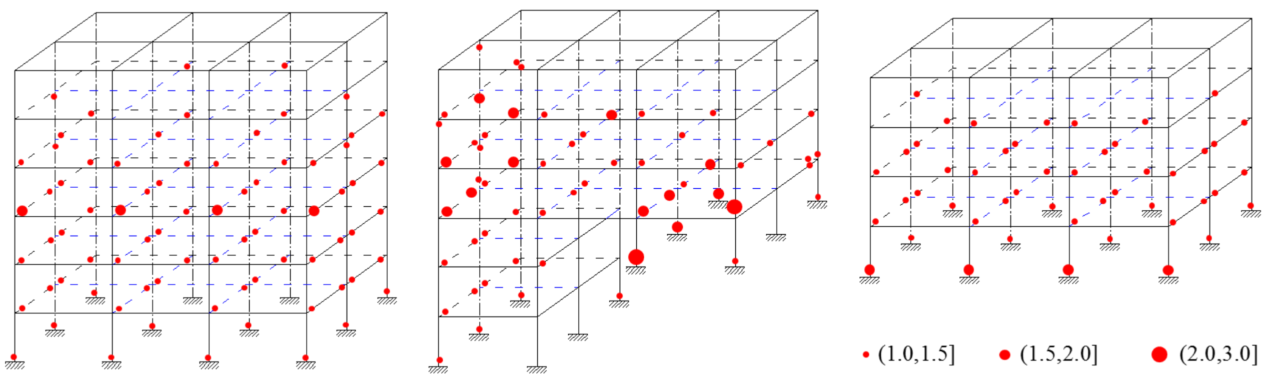

a) M-6 b) M-D2K1 c) M-4

Fig. 8 – Plastic hinges of frame structure models under the action of ground motion record 13 with intensity of 0.40g along Y axis

Fig. 8 shows plastic hinges of frame structure models under rare earthquake with intensity of 0.40g along Y axis. Plastic hinges are mainly at the end of columns and beams along Y axis except one beam at 3rd floor along X axis. In common frame structure M-4 and M-6, the bottom of columns at 1st floor are all hinged, and the rest plastic hinges are mainly located at beams ends. In step-back frame structure M-D2K1, there are plastic hinges at bottom of columns connected with lower embedding end and columns connected with upper embedding end, and the damage at bottom of columns connected with upper embedding end is worse. The damage degree of beam ends on higher floors at side of columns connected with lower embedding end is greater.

In order to investigate the development of plastic hinges of step-back frame structure, time history analysis with intensity of 0.62g was performed. Fig. 9 presents the distribution of plastic hinges of M-D2K1 under the action of ground motion record 13. It is clearly that the quantity and degree of plastic hinges increase markedly. In the along-slope direction, the damage degree of the bottom of columns connected with upper embedding end increases significantly, so do beams connected with these columns. Plastic hinges occur at ends of beams at 2nd floor. The damage still mainly distribute at end of components at floors above upper embedding end, and most of columns at 5th floor are hinged at the top. In the across-slope direction, the damage of columns connected with upper embedding end and beams connected with them is enhanced. Also, plactic hinges occur at top of all columns at 5th floor.

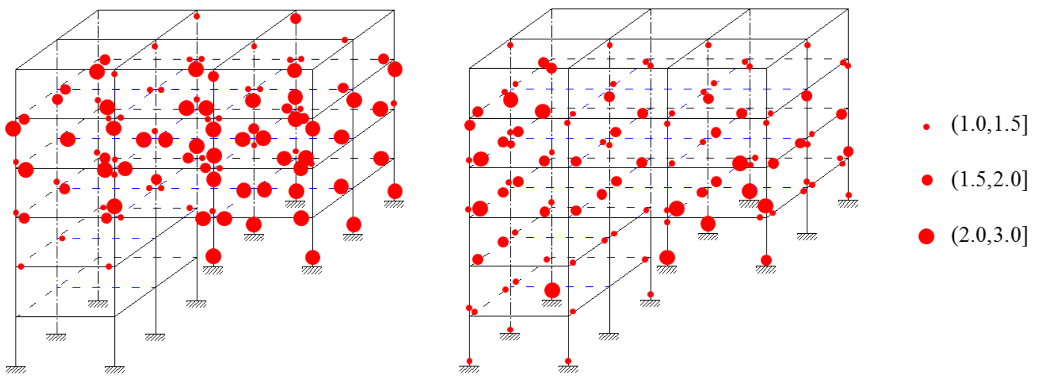

a) Along the slope b) Across the slope

Fig. 9 – Plastic hinges of step-back frame structure model under the action of ground motion record 13 with intensity of 0.62g

6 Conclusions

The step-back frame structure has significant torsion effect, and the deformation and force characteristic of step-back frame structure is different from that of common frame. The deformation of step-back deformation is between that of the corresponding common structures.

The distribution of plastic hinges of step-back frame structure is different from common frame structure, and in step-back frame structure, there is an obvious difference in the along-slope and across-slope direction.

Under the action of rare earthquake, common frame structures show typical beam hinge mechanisms. In the along-slope direction of step-back frame structure, columns connected with upper embedding end are damaged severely, and components at floors under upper embedding end are no damage. In the across-slope direction, the embedding columns at two sides are damaged. The damage mechanisms of step-back frame structure is different from that of common frame structure. When a stronger earthquake is subjected, the damage at floors below upper embedding end increases.

7 Acknowledgements

The research in this paper was supported by the National Natural Science Foundation of China (Nos. 51638002 and 51878101).

8 References

[1] Liping W, Yingmin L, Nina Z, et al. (2009): Seismic damage investigation on typical slope building in Wenchuan Earthquake. *Journal of Xi'an University of Architecture & Technology (Natural Science Edition)*, **41** (6), 822-826.

[2] Narayanan ARV, Goswami R, Murty CVR (2014): Performance of RC buildings along hill slopes of Himalayas during 2011 Sikkim earthquake. *15th World Conference of Earthquake Engineering WCEEXV*. Lisboa, Portugal.

[3] Singh Y, Gade P, Lang DH, et al. (2014): Seismic behavior of buildings located on slopes - an analytical study and some observations from Sikkim earthquake of September 18, 2011. *15th World Conference of Earthquake Engineering WCEEXV*. Lisboa, Portugal.

[4] Yao Z (2011): Study on Dynamic Characteristics and Overturning Stability for Structures Supported by Foundations with Different Horizontal Levels. Master thesis, Chongqing University, Chongqing, China.

[5] Cunxiong W (2017): Study on seismic design of step-terrace structure based on failure control. Master thesis, Chongqing University, Chongqing, China.

[6] Liping L, Anliang L, Yingmin L, et al. (2014): Feasibility of torsional control index in frame structure with uneven height grounding column ends. *Earthquake Engineering and Engineering Dynamic*, **34** (S1), 680-685.

[7] Xianbo T (2015): Seismic Damage Mechanism of RC Frame Stuctures on the Slope. Master thesis, Chongqing University, Chongqing, China.

[8] Scott BD, Park R, Priestley MJN (1982): Stress-Strain Behavior of Concrete Confined by Overlapping Hoops at Low and High Strain Rates. *Journal of the American Concrete Institute*, **79** (1), 13-27.

[9] Park R, Paulay T (1975): *Reinforced concrete structures*. Wiley, 1st edition.

[10] Pu Y, Yingmin L, Ming L (2000): A new method for selecting inputting waves for time-history analysis. *China Civil Engineering Journal*, **33** (6), 33-37.

